

Green, homogeneous oxidation of alcohols by dimeric copper(II) complexes

Abhishek Maurya & Chanchal Haldar

To cite this article: Abhishek Maurya & Chanchal Haldar (2020): Green, homogeneous oxidation of alcohols by dimeric copper(II) complexes, Journal of Coordination Chemistry, DOI: [10.1080/00958972.2020.1857747](https://doi.org/10.1080/00958972.2020.1857747)

To link to this article: <https://doi.org/10.1080/00958972.2020.1857747>

 View supplementary material [↗](#)

 Published online: 17 Dec 2020.

 Submit your article to this journal [↗](#)

 View related articles [↗](#)

 View Crossmark data [↗](#)



Green, homogeneous oxidation of alcohols by dimeric copper(II) complexes

Abhishek Maurya  and Chanchal Haldar 

Department of Chemistry, Indian Institute of Technology (Indian School of Mines), Dhanbad, Jharkhand, India

ABSTRACT

Three pyrazole derivatives, 3,5-dimethyl-1*H*-pyrazole (DMPz) (**I**), 3-methyl-5-phenyl-1*H*-pyrazole (MPPz) (**II**), and 3,5-diphenyl-1*H*-pyrazole (DPPz) (**III**), were prepared via reacting semicarbazide hydrochloride with the acetylacetone, 1-phenylbutane-1,3-dione, and 1,3-diphenylpropane-1,3-dione, respectively. Complexes **1–3** were isolated by reacting $\text{CuCl}_2 \cdot 2\text{H}_2\text{O}$ with **I–III**, respectively, and characterized by CHNS elemental analyses, FT-IR, UV-Vis, ^1H and ^{13}C NMR, EPR spectra, and TGA/DTA. Molecular structures of the pyrazole derivatives **I–III** and copper(II) complexes **2** and **3** were studied through single-crystal XRD analysis to confirm their molecular structures. Overlapping of hyperfine splitting in the EPR spectra of the dimeric copper(II) complexes **1–3** indicates that both copper centers do not possess the same electronic environment in solution. The copper(II) complexes are dimeric in solid state as well as in solution and catalyze the oxidation of various primary and secondary alcohols selectively. Catalysts **1–3** show more than 92% product selectivity toward ketones during the oxidation of secondary alcohols. Surprisingly primary alcohols, which are relatively difficult to oxidize, produce carboxylic acid as a major product (48%–90% selectivity) irrespective of catalytic systems. The selectivity for carboxylic acid rises with decreasing the carbon chain length of the alcohols. An eco-friendly and affordable catalytic system for oxidation of alcohols is developed by the utilization of H_2O_2 , a green oxidant, and water, a clean and greener solvent, which is a notable aspect of the study.

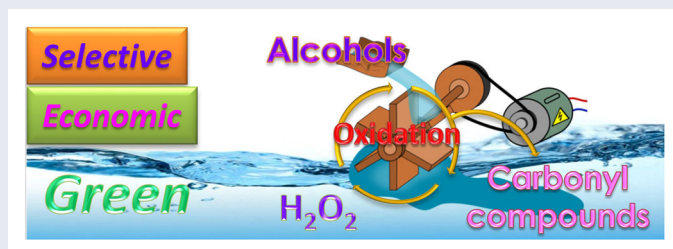
ARTICLE HISTORY

Received 30 June 2020

Accepted 12 November 2020

KEYWORDS

Homogeneous catalysis; copper complexes; pyrazole derivatives; EPR; alcohol oxidation



CONTACT Chanchal Haldar  chanchal@iitism.ac.in  Department of Chemistry, Indian Institute of Technology (Indian School of Mines), Dhanbad-826004, Jharkhand, India

 Supplemental data for this article is available online at <https://doi.org/10.1080/00958972.2020.1857747>.

© 2020 Informa UK Limited, trading as Taylor & Francis Group

1. Introduction

Aldehydes, ketones, and carboxylic acids represent “the class of valuable chemicals” in current industrial and synthetic chemistry, and demands for these chemicals are growing. These compounds are used as solvents, perfumes, and flavoring agents or critical intermediates for the synthesis of other important compounds [1]. To meet the demands, catalytic oxidation of alcohols to carbonyl compounds is the most common pathway. A variety of oxidation processes like Dess–Martin oxidation [2], Swern oxidation [3], Jones oxidation [4], Oppenauer oxidation [5], or traditional stoichiometric oxidants, such as chromium oxide, have been reported. Despite the use of toxic chemicals, the generation of a large number of by-products, and inherent safety issues, large-scale manufacturing of carbonyl compounds from alcohols are still using these methods [6]. In order to find out an inexpensive, uncomplicated, waste-free, and green method for transformation of alcohols into carbonyl compounds, transition of metal-catalyzed alcohol oxidation is continuously evolving [7]. Three aspects need to be addressed to make the selective catalytic oxidation of alcohol economical and green: a straightforward and facile synthesis of catalysts with inexpensive raw materials; the use of greener and safer oxidizing agents; use of clean and green solvent.

Copper-based catalytic systems are economical due to their high natural abundance and lower price. The catalytic properties of copper complexes are also unquestionable. Among the variety of other transition metals, copper occupies a special place in connection with the development of greener and economic catalysts for the transformation of alcohol into carbonyl compounds. Copper can be found in the active site of monometallic enzymes [8], bimetallic enzymes [9], multimetallic enzymes [10], or even in heterometallic enzymes [11]. A number of catalytic systems have been reported where molecular oxygen or hydrogen peroxide were used as greener oxidants. Using atmospheric oxygen as an oxidant in alcohol oxidation is an excellent choice, but hydrogen peroxide as an oxidant has its advantages over atmospheric oxygen. In large-scale production of carbonyl compounds from alcohol, handling, transportation, and the use of gaseous oxygen can be problematic [12]. A variety of transition metal-catalyzed alcohol oxidations in the presence of hydrogen peroxide have been reported [13], where organic solvent dissolves these catalysts making the recovery of the catalysts difficult. Therefore, the concept of economic and green process fails.

A number of reports deal with copper-catalyzed aerobic oxidation [14]. However, transition metal-catalyzed alcohol oxidation using hydrogen peroxide as an oxidant started getting momentum in the last decade. A number of reports of heterogeneous [15] copper-based catalysts using hydrogen peroxide as an oxidant are available, but similar homogeneous systems are scarce [7(c), 16].

Here, we explore the catalytic potential of three dimeric copper(II) complexes of pyrazole derivatives, 3,5-dimethyl-1*H*-pyrazole (DMPz) (**I**), 3-methyl-5-phenyl-1*H*-pyrazole (MPPz) (**II**), and 3,5-diphenyl-1*H*-pyrazole (DPPz) (**III**), for selective oxidation of alcohols in the presence of hydrogen peroxide. Pyrazole derivatives **I–III** and their corresponding copper(II) complexes, $[\text{Cu}(\text{DMPz})_2\text{Cl}_2]_2$ (**1**), $[\text{Cu}(\text{MPPz})_2\text{Cl}_2]_2$ (**2**), and $[\text{Cu}(\text{DPPz})_2\text{Cl}_2]_2$ (**3**), are reported separately in a number of articles [17]. Pyrazole and its derivatives are principal components of various pharmaceutical and agrochemical products such as anti-inflammatories, anticoagulants, and antimicrobials [18]. Pyrazole

derivatives are synthesized by reacting 1,3-dicarbonyl compounds with hydrazine derivatives. In 1951, Wiley and Hexner reported the synthesis of DMPz, where hydrazine sulfate was dissolved in aqueous sodium hydroxide and reacted with acetylacetone in ethanol. Compounds were extracted from the reaction mixture with ether and recrystallized in petroleum ether with a 73% yield [19]. The reaction of acetylacetone with hydrazine hydrate in ethanol is an alternative route for the synthesis of DMPz. However, the reaction with hydrazine hydrate is violent. Therefore the earlier method is more acceptable. Hydrolysis and decarboxylation of 1-carbamido- or 1-carboxamide derivatives also lead to the formation of DMPz [20]. The 1-carbamido derivatives are easily prepared by reacting semicarbazide or aminoguanidine with acetylacetone [21], and 1-carboxamidine derivatives can be prepared from 1,2-pentadiene-4-one and hydrazine hydrate [22]. The synthesis of DPPz was reported by Kitajima *et al.* in 1992. Hydrazine hydrate was added dropwise into the ethanolic solution of dibenzoylmethane, and after 30 min of refluxing a white product with 85% yield was collected by filtration [23]. In 2013, Lee *et al.* reported the solid-phase synthesis of pyrazole derivatives, including DMPz, MPPz, and DPPz, where 1,3-dicarbonyl derivatives were reacted with solid hydrazine at 70 °C for 2 h. The isolated yields of DMPz, MPPz, and DPPz are 99%, 98%, and 98%, respectively [24]. Here, we have adopted a simple, single-step method for preparation of **I–III**. We replaced reactive hydrazine hydrate with semicarbazide hydrochloride, which is the major difference from the reported synthetic methods. After completion of the reaction, the three pyrazole derivatives were isolated as single crystals. Chandrasekhar *et al.* first reported the synthesis of $[\text{Cu}(\text{DMPz})_2\text{Cl}_2]_2$ by the complete desulfurization of bis(3,5-dimethyl pyrazolyl)methylphosphine sulfide ($\text{MeP}(\text{S})(3,5\text{-Me}_2\text{Pz})_2$) followed by hydrolysis of P-N bonds. The reaction of $\text{MeP}(\text{S})(3,5\text{-Me}_2\text{Pz})_2$ with anhydrous CuCl_2 in 1:1 ratio produces $[\text{Cu}(\text{DMPz})_2\text{Cl}_2]_2$ along with a tetranuclear copper complex $[\text{Cu}_2\text{Cl}_2(3,5\text{-Me}_2\text{Pz})_3(\text{MePO}_3)_2]$. These two complexes were separated by recrystallization from a mixture of CH_2Cl_2 and hexane [17(c)]. In 2015, Giles *et al.* reported the synthesis of the same compounds by reacting 3,5-dimethylpyrazole with $\text{CuCl}_2 \cdot 2\text{H}_2\text{O}$ in an aqueous medium [17(e)]. However, Chandrasekhar *et al.* did not mention the yield of $[\text{Cu}(\text{DMPz})_2\text{Cl}_2]_2$, but Giles *et al.* isolated the complex with 94% yield. In 2012, Soltani and co-workers first established the synthesis and structure of $[\text{Cu}(\text{MPPz})_2\text{Cl}_2]_2$. The compound was isolated (75% yield) from the reaction of DPPz with anhydrous CuCl_2 in a mixture of acetonitrile and methanol (1:1) for 12 h [17(f)]. Mezei and co-workers reported the synthesis of $[\text{Cu}(\text{DPPz})_2\text{Cl}_2]_2$ by reacting DPPz with $\text{CuCl}_2 \cdot 2\text{H}_2\text{O}$ in the presence of 1 equivalent of NaOH. Recrystallization from layering a THF solution with hexane produced single crystals (57% yield), confirming the molecular structure [17(d)]. All three copper(II) complexes (**1–3**) are characterized only by FT-IR, UV-Vis spectroscopy, and single-crystal XRD analysis [17]. No other techniques were used to analyze the properties of **1–3**. Here, we have further analyzed these complexes by using EPR (electron paramagnetic resonance) spectroscopy and thermogravimetric analysis (TGA). There are no reports on application of these complexes. Hence, we have utilized **1–3** for the catalytic oxidation of primary and secondary alcohols.

Copper complexes **1–3** were synthesized by a straightforward, faster, and single-step method by reacting pyrazole derivatives DMPz (**I**), MPPz (**II**), and DPPz (**III**) with $\text{CuCl}_2 \cdot 2\text{H}_2\text{O}$ in refluxing methanolic solution for 2 h. After the reaction, **2** and **3** were

separated as single crystals from the reaction mixture, whereas **1** was isolated in powder form.

We have used water, a green solvent, during the catalytic oxidation of alcohol in the presence of **1–3**. In order to make the catalytic process economical, safe, and green, hydrogen peroxide was used as an oxidant. The scope of the alcohol oxidation was increased by using a variety of cyclic, acyclic aliphatic alcohols, and aromatic alcohols. Despite the inherent difficulties associated with the oxidation of primary alcohols, **1–3** showed excellent catalytic performance in terms of conversion as well as selectivity. Secondary alcohols converted into ketones with almost 100% selectivity irrespective of catalyst, but primary alcohols produced carboxylic acids as the major product. Interestingly, the carboxylic acid selectivity increases with decreasing the carbon chain length of the alcohol.

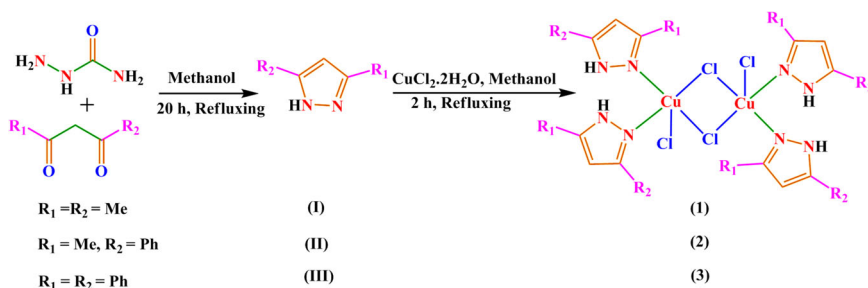
2. Experimental

2.1. Materials

Acetyl acetone (Merck, India), benzoyl acetone (Alfa-Aesar, India), 1,3-diphenyl-1,3-propanedione (Sigma-Aldrich, USA), semicarbazide hydrochloride (Avra, India), $\text{CuCl}_2 \cdot 2\text{H}_2\text{O}$ (Loba-Chemie, India), benzyl alcohol (Merck, India), 1-heptanol (TCI, Japan), 1-hexanol (Alfa-Aesar, India), 1-pentanol (TCI, Japan), cyclohexanol (Alfa-Aesar, India), 1-butanol (TCI, Japan), 1-propanol (TCI, Japan), 2-propanol (Merck, India), 2-butanol (TCI, Japan), 30% H_2O_2 (Merck, India), TBHP (Alfa-Aesar, India), deionized water, and AR-grade solvent (Merck & Rankem, India) were used as received. HPLC-grade methanol and ethyl acetate (Spectrochem, India) were used for GC analysis.

2.2. Physical methods and analysis

FT-IR spectra of the ligands and their copper complexes were recorded on an Agilent Cary 600 Series FT-IR spectrometer by the ATR (attenuated total reflection) method. Electronic spectra of the ligands and Cu(II) complexes were recorded with a SHIMADZU UV-1800 spectrophotometer using methanol/DMF as solvent. The ^1H and ^{13}C NMR spectra of the pyrazole derivatives were recorded with a Bruker AC-400 NMR spectrometer using $\text{DMSO-}d_6/\text{CDCl}_3$ as a solvent with standard parameter settings. Waters Q-ToF Micromass was used for ESI^+ -MS of metal complexes. TGA and differential thermal analysis (DTA) were performed with a PerkinElmer, Diamond TG/DTA instrument. X-band EPR spectra of the copper(II) complexes were recorded in a JES-FA200 ESR spectrometer at 77 K. The single-crystal data of ligands and their respective copper complexes were collected by the Rigaku Oxford Diffraction system equipped with a state of the art CCD Eos S2 detector using $\text{Mo K}\alpha$ radiation (wavelength 0.71073 Å) at room temperature. Catalytic oxidations of various alcohols and alkenes were monitored by an Agilent gas-chromatograph (7890B) fitted with an HP-5 capillary column (30 m \times 0.32 mm \times 0.25 μm) and an FID detector. Catalytic oxidation products of alcohols were identified by comparing with commercially available standards in GC. The confirmation of prepared pyrazoles **I–III** and oxidation products was done



Scheme 1. Proposed synthetic route for synthesis of 3,5-dimethyl-1*H*-pyrazole (DMPz) (I), 3-methyl-5-phenyl-1*H*-pyrazole (MPPz) (II), and 3,5-diphenyl-1*H*-pyrazole (DPPz) (III) and their corresponding copper complexes $[\text{Cu}(\text{DMPz})_2\text{Cl}_2]_2$ (1), $[\text{Cu}(\text{MPPz})_2\text{Cl}_2]_2$ (2), and $[\text{Cu}(\text{DPPz})_2\text{Cl}_2]_2$ (3).

by GC-MS (Trace 1300 ISQ QD) with a TG-5MS capillary column (30 m \times 0.25 mm \times 0.25 μm) and an EI^+ -Mass detector.

2.3. Synthesis

2.3.1. Synthesis of pyrazole derivatives: 3,5-dimethyl-1*H*-pyrazole (DMPz) (I), 3-methyl-5-phenyl-1*H*-pyrazole (MPPz) (II) and 3,5-diphenyl-1*H*-pyrazole (DPPz) (III)

Synthesis of DMPz (I) has been known for a long time. A number of reports can be found in the literature describing the synthesis of I–III [19, 24, 25]. Solution phase synthesis of I–III was done by simplifying the method described in the literature [19]. A mixture of 20 mL methanolic solution of semicarbazide hydrochloride (1.11 g, 10 mmol) and 20 mL methanolic solution of acetylacetone (1.00 g, 10 mmol) was refluxed for ~ 20 h (Scheme 1) with constant stirring. The volume of the final solution was reduced to ~ 10 mL and kept in a refrigerator overnight. White crystals suitable for single-crystal X-ray analysis separated. Crystals were filtered, washed with cold methanol, and dried in vacuum over silica gel.

By following the same synthetic procedure as described above, we isolated MPPz (II) and DPPz (III) by replacing acetylacetone with 1-phenylbutane-1,3-dione and 1,3-diphenylpropane-1,3-dione, respectively. All three pyrazoles were isolated as single crystals from the reaction mixture. The straightforward and single-step process with easy product separation (as single crystals) makes the current synthetic route preferable among the other synthetic methods reported.

Data for DMPz (I): Yield: 0.50 g (53%); Anal. Calcd for $\text{C}_5\text{H}_8\text{N}_2$ (MW 96.13); C, 62.47%; H, 8.39%; N, 29.14%. Found: C, 61.98%; H, 8.21%; N, 29.55%. FT-IR (ATR, cm^{-1}): 3194 and 3119 ($\nu_{\text{N-H}}$), 1596 ($\nu_{\text{C=N}}$), 1520 ($\nu_{\text{C=C}}$); UV-Vis [λ_{max} (nm), ϵ ($\text{Lmol}^{-1}\text{cm}^{-1}$)]: 219 (2.98×10^4); ^1H NMR (DMSO- d_6 , δ in ppm): 2.2 (s, 6H), 5.9 (s, 1H), 13.1 (s, 1H); ^{13}C NMR (DMSO- d_6 , δ in ppm): 10.6, 106.0, 144.4; EI^+ -MS of I: m/z experimental = 96.16, observed = 96.13 ($[\text{DMPz}]^+$).

Data for MPPz (II): Yield: 0.92 g (58%); Anal. Calcd for $\text{C}_{10}\text{H}_{10}\text{N}_2$ (MW 158.20); C, 75.92%; H, 6.37%; N, 17.71%. Found: C, 75.98%; H, 7.09%; N, 18.11%. FT-IR (ATR, cm^{-1}): 3176 and 3127 ($\nu_{\text{N-H}}$), 1606 ($\nu_{\text{C=N}}$), 1533 ($\nu_{\text{C=C}}$); UV-Vis [λ_{max} (nm), ϵ ($\text{Lmol}^{-1}\text{cm}^{-1}$)]: 255 (2.95×10^4); ^1H NMR (CDCl_3 , δ in ppm): 2.3 (s, 3H), 6.8 (s, 1H), 7.3–7.4 (m, 3H), 7.8–7.9 (m, 2H), 14.1 (s, 1H); ^{13}C NMR (DMSO- d_6 , δ in ppm): 11.4, 103.4, 126.9, 127.0, 129.3,

130.4, 145.2, 147.2; EI⁺-MS of **II**: m/z experimental = 158.18, observed = 158.20 ([MPPz]⁺).

Data for DPPz (III): Yield: 1.06 g (48%); Anal. Calcd for C₁₅H₁₂N₂ (MW 220.27); C, 81.79%; H, 5.49%; N, 12.72%. Found: C, 81.58%; H, 5.21%; N, 12.55%. FT-IR (ATR, cm⁻¹): 3201 and 3120 (ν_{N-H}), 1602 (ν_{C=N}), 1531 (ν_{C=C}); UV-Vis [λ_{\max} (nm), ϵ (Lmol⁻¹cm⁻¹)]: 251 (1.71 × 10⁴); ¹H NMR (DMSO-d₆, δ in ppm): 7.0 (s, 1H), 9.7 (s, 1H), 7.2–7.3 (m, 2H), 7.4–7.4 (m, 4H), 7.8–7.8 (s, 4H); ¹³C NMR (DMSO-d₆, δ in ppm): 100.7, 125.9, 129.0, 129.2, 130.0, 147.4, 158.0; EI⁺-MS of **III**: m/z experimental = 220.20, observed = 220.27 ([DPPz]⁺).

2.3.2. Synthesis of [Cu(DMPz)₂Cl₂]₂ (**1**), [Cu(MPPz)₂Cl₂]₂ (**2**) and [Cu(DPPz)₂Cl₂]₂ (**3**)

Complexes **1–3** were prepared by following a simple synthetic route (presented in Scheme 1). CuCl₂·2H₂O (1.70 g, 10 mmol) was refluxed (~70 °C) with **I–III** in a 1:2 ratio in 40 mL of methanol for 2 h with constant stirring. A blue precipitate for **1**, greenish crystals for **2**, and dark blue crystals of **3** were separated from the refluxing reaction mixture, which was filtered, washed with methanol (3 × 10 mL), and dried in vacuum over silica gel.

Data for [Cu(DMPz)₂Cl₂]₂ (1**):** Yield: 2.93 g (44%); Anal. Calcd for C₂₀H₃₂Cl₄Cu₂N₈ (MW 650.01); C, 36.76%; H, 4.94%; N, 17.15%. Found: C, 36.88%; H, 5.10%; N, 17.35%. FT-IR (ATR, cm⁻¹): 3147 and 3040 (ν_{N-H}), 1583 (ν_{C=N}); UV-Vis [λ_{\max} (nm), ϵ (Lmol⁻¹cm⁻¹)]: 236 (sh), 271 (4.09 × 10⁴); ESI⁺-MS of **1**: calculated m/z = 256.86, observed = 256.81 ([Cu(DMPz)₂] + H)⁺.

Data for [Cu(MPPz)₂Cl₂]₂ (2**):** Yield: 3.15 g (35%); Anal. Calcd for C₄₀H₄₀Cl₄Cu₂N₈ (MW 901.70); C, 53.28%; H, 4.47%; N, 12.43%. Found: C, 53.48%; H, 4.71%; N, 12.55%. FT-IR (ATR, cm⁻¹): 3240 and 3134 (ν_{N-H}), 1583 (ν_{C=N}); UV-Vis [λ_{\max} (nm), ϵ (Lmol⁻¹cm⁻¹)]: 207 (2.64 × 10⁴), 256 (1.66 × 10⁴); ESI⁺-MS of **2**: calculated m/z = 381.10, observed = 380.95 ([Cu(MPPz)₂] + H)⁺.

Data for [Cu(DPPz)₂Cl₂]₂ (3**):** Yield: 6.50 g (53%); Anal. Calcd for C₅₈H₄₇Cl₄Cu₂N₈ (MW 1124.94); C, 62.67%; H, 4.21%; N, 9.74%. Found: C, 62.52%; H, 4.19%; N, 9.63%. FT-IR (ATR, cm⁻¹): 3246 and 3212 (ν_{N-H}), 1593 (ν_{C=N}); UV-Vis [λ_{\max} (nm), ϵ (Lmol⁻¹cm⁻¹)]: 252 (1.63 × 10⁴); ESI⁺-MS of **3**: calculated m/z = 505.22, observed = 505.09 ([Cu(DPPz)₂] + H)⁺.

2.4. Oxidation of alcohols

The homogeneous catalytic oxidations of alcohols were carried out using **1**, **2**, and **3** in a 50 mL double-neck round bottom flask fitted with a water circulated condenser. Conventionally benzyl alcohol (1.08 g, 10 mmol), 30% aqueous H₂O₂ (9.07 g, 80 mmol), and catalyst (7 mg) were mixed in 7.5 mL of water and heated for 6 h with constant stirring. A small aliquot of the reaction mixture was withdrawn periodically, extracted with ethyl acetate, and analyzed with a GC fitted with an HP-5 column. The identity of oxidation products was confirmed by comparing with commercially available standards and GC-MS. To achieve the maximum substrate conversion(%), all the measurable reaction parameters such as catalysts amount, oxidant amount, nature of oxidant, solvent amount, types of solvent, and temperature were carefully optimized.

3. Results and discussion

Ligands **I–III** and copper(II) complexes **1–3** were analyzed by FT-IR and UV-Vis spectroscopy, which is comparable with the data reported [17]. All the FT-IR and UV-Vis spectra are shown in [Supplementary Figures S1–S3](#), and selected FT-IR data are summarized in [Supplementary Table S1](#). The pyrazole derivatives **I–III** were further characterized by ^1H and ^{13}C NMR spectroscopy. All the data are in accordance with reported data [26]. The ^1H and ^{13}C NMR spectra of **I–III** are shown in [Supplementary Figures S4 and S5](#), and the appropriate assignment of these signals along with the detailed chemical shifts are tabulated in [Supplementary Tables S2 and S3](#). Prepared pyrazole derivatives DMPz (**I**), MPPz (**II**), and DPPz (**III**) along with copper(II) complexes $[\text{Cu}(\text{MPPz})_2\text{Cl}_2]_2$ (**2**) and $[\text{Cu}(\text{DPPz})_2\text{Cl}_2]_2$ (**3**) were crystallized and analyzed through single-crystal X-ray crystallography. ORTEP plots of **I–III**, **2**, and **3** are displayed in [Supplementary Figures S6 and S7](#) with 50% thermal ellipsoids. The detailed crystallographic data of **I–III** along with **2** and **3** are summarized in [Supplementary Table S4](#). All the single-crystal X-ray analysis data confirm the molecular structures of **I–III**, **2**, and **3**.

3.1. EPR spectral analysis

Frozen DMF solution X-band EPR spectra of $[\text{Cu}(\text{DMPz})_2\text{Cl}_2]_2$ (**1**), $[\text{Cu}(\text{MPPz})_2\text{Cl}_2]_2$ (**2**) and $[\text{Cu}(\text{DPPz})_2\text{Cl}_2]_2$ (**3**) are shown in [Figure 1](#). All the spectra are characteristic of an axially symmetrical paramagnetic Cu^{2+} center and display a well resolved parallel region but unresolved perpendicular region.

In solution, **1–3** show $g_{\parallel} > g_{\perp} > g$ (2.0023), which is characteristic of a distorted square pyramidal copper(II) center where the $d_{x^2-y^2}$ orbital carries the unpaired electron [27]. Interaction of copper(II) nuclear spin ($I = 3/2$) with the spin of its unpaired electron ($S = 1/2$) causes the hyperfine splitting in the EPR spectra of **1–3** with an average splitting of 128 G, 122 G, and 112 G, respectively. Each of the peaks in the parallel region appears split in two, suggesting that the mutual overlapping of the hyperfine structures of the two copper(II) centers of the dimeric complexes **1–3** causes splitting in the peaks [27(a,b)]. Also, it indicates that both copper centers in the dimeric copper(II) complexes **1–3** are not magnetically equivalent. Lack of forbidden $\Delta M_s = \pm 2$ transition, at the half field, eliminates the possibility of interaction among the two copper(II) centers in the dimeric complexes. The calculated EPR parameters for **1–3** are listed in [Table 1](#).

3.2. Thermal analysis

The thermal stabilities of copper(II) complexes $[\text{Cu}(\text{DMPz})_2\text{Cl}_2]_2$ (**1**), $[\text{Cu}(\text{MPPz})_2\text{Cl}_2]_2$ (**2**) and $[\text{Cu}(\text{DPPz})_2\text{Cl}_2]_2$ (**3**) were examined by TGA/DTA under a nitrogen atmosphere from 30 to 900 °C at 10 °C/min as shown in [Figure 2](#).

Complexes **1** and **2** follow a three-step exothermic decomposition process, while **3** shows a two-step exothermic decomposition pattern. Decomposition steps are clear in **1**, whereas **2** and **3** show overlapping steps during the entire temperature range. Initial mass losses in **1–3** start around 100 °C and continue until 180 °C in **1** and **2**,

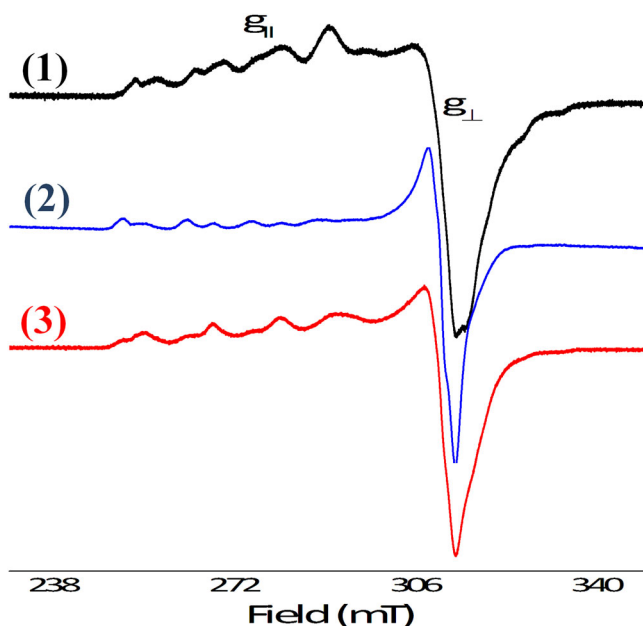


Figure 1. X-band EPR spectra of **1**, **2**, and **3** recorded in DMF at 77 K.

Table 1. Data of spin Hamiltonian parameters of **1–3** in DMF solution at 77 K.

Property	1		2		3	
	$A_{ }$					
$g_{ }$	2.3728	128 G	2.3949	122 G	2.4020	112 G
g_{\perp}	2.0948		2.0874		2.0890	

and up to 240 °C for **3**. During this, **1–3** mostly eliminate adsorbed moisture and entrapped solvent molecules. In the second step, **1** loses chloride in the temperature range of 200 to 295 °C. In the third and final step, **1** undergoes a massive 54.45% mass loss from 300 to 620 °C due to complete breakdown of the organic component, leaving CuO as final product. However, in **2** and **3**, elimination of chloride and decomposition of organic components start in an overlapping manner. In **2**, 64.94% mass loss was observed in the second step, followed by a 10.18% mass loss in the final step. In its second and final step, **3** displays 73.99% weight loss. From the TGA plots complexes **1–3** are thermally stable up to 200, 181, and 180 °C, respectively, which is sufficient to use copper(II) complexes as catalysts under moderate temperature without losing their molecular structures.

4. Catalytic activity

4.1. Alcohol oxidation

Despite their well-known molecular structures [17], [Cu(DMPz)₂Cl₂]₂ (**1**), [Cu(MPPz)₂Cl₂]₂ (**2**) and [Cu(DPPz)₂Cl₂]₂ (**3**) have not been examined as catalysts. The catalytic potential of **1–3** is investigated for the liquid phase oxidation of a series of alcohols (listed in

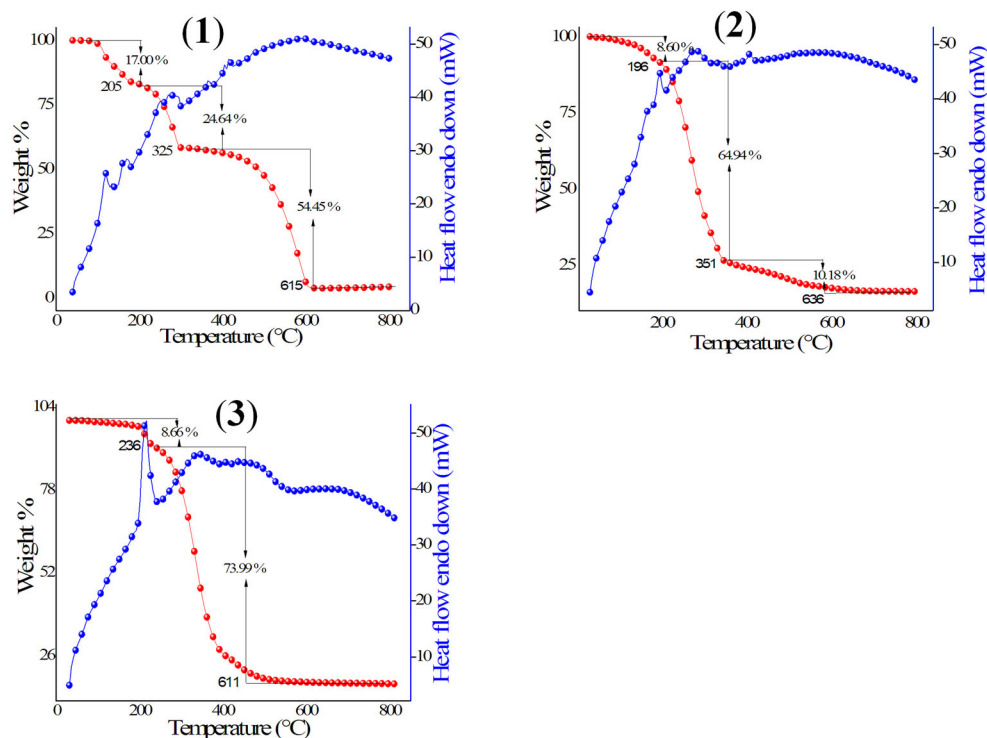


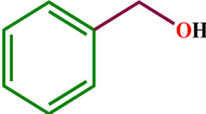
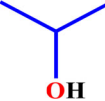
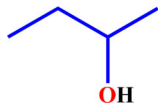
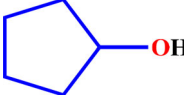
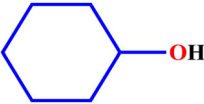
Figure 2. TGA/DTA plot of $[\text{Cu}(\text{DMPz})_2\text{Cl}_2]_2$ (1), $[\text{Cu}(\text{MPPz})_2\text{Cl}_2]_2$ (2), and $[\text{Cu}(\text{DPPz})_2\text{Cl}_2]_2$ (3).

Table 2) in the presence of H_2O_2 under moderate reaction conditions. The reaction parameters were optimized to obtain the maximum substrate conversion (%). During the optimization of the reaction parameters, **3** was used as a model catalyst and benzyl alcohol was used as a representative substrate.

To optimize the amount of catalyst, four different amounts, i.e. 0.001 g, 0.003 g, 0.005 g, and 0.007 g were used in the presence of a fixed amount of benzyl alcohol (1.08 g, 10 mmol), 30% H_2O_2 (3.40 g, 30 mmol), and solvent (10 mL, 7 mL H_2O mixed with 3 mL of methanol) at 100°C (shown in Figure 3(A)). After 6 h of reaction time, 0.001 g of catalyst shows only 12.5% of conversion. With increasing amount of catalyst, substrate conversion increases progressively. A maximum of 28.3% conversion was achieved by using 0.007 g of catalyst. Hence, 0.007 g of catalyst was chosen as optimum.

The impact of the amount of oxidant in the oxidation of benzyl alcohol was studied by employing six different substrates to oxidant ratio, i.e. 1:3, 1:4, 1:5, 1:6, 1:7, and 1:8 while keeping other reaction parameters constant; six reactions were carried out where a fixed amount of benzyl alcohol was reacted with different oxidant amounts. In each reaction, 1.08 g of benzyl alcohol was reacted with 3.40 g, 4.53 g, 5.66 g, 6.8 g, 7.93 g, or 9.06 g of 30% H_2O_2 . It is evident from Figure 3(B) that by increasing the substrate to oxidant ratio from 1:3 to 1:8, substrate conversion also improves steadily. Therefore, 1:8 substrate to oxidant ratio was set as optimum as it produces a maximum of 58.4% of conversion in 6 h.

Table 2. Catalytic data for the oxidation of alcohols in the presence of 1–3 under the optimized reaction conditions.

S. No.	Cat.	Substrate	% Conv.	TOF (h ⁻¹)	Selectivity (%)	
					-CHO/>C=O	-COOH
1	1		83.2	64.72	12.28	79.47
	2		66.4	71.27	12.48	80.94
	3		81.2	111.16	13.94	78.17
	Blank				12.7	
2	1		41.8	32.51	20.46	61.48
	2		30.7	32.95	25.10	58.25
	3		37.4	51.20	22.78	59.98
	Blank				5.9	
3	1		49.2	38.27	24.34	54.34
	2		46.4	49.80	32.99	50.03
	3		58.4	79.95	15.44	58.78
	Blank				8.5	
4	1		51.0	39.67	26.84	48.49
	2		49.4	53.02	5.67	50.89
	3		42.0	57.49	24.46	52.34
	Blank				7.3	
5	1		50.3	39.12	19.81	67.89
	2		32.7	35.10	12.65	75.46
	3		25.6	35.04	12.30	76.57
	Blank				4.5	
6	1		74.2	57.71	14.77	81.78
	2		58.2	62.47	9.90	87.54
	3		48.4	66.26	6.94	90.72
	Blank				5.4	
7	1		52.6	40.91	92.78	7.22
	2		49.4	53.02	95.49	4.51
	3		48.2	65.98	95.88	4.12
	Blank				6.8	
8	1		88.2	68.61	98.98	1.02
	2		80.1	85.98	99.39	0.61
	3		77.6	106.23	100	0.00
	Blank				9.8	
9	1		57.5	44.72	98.20	1.80
	2		53.0	56.89	98.89	1.11
	3		56.6	77.48	98.29	1.71
	Blank				7.2	
10	1		37.0	28.78	97.68	2.32
	2		47.2	50.66	95.98	4.02
	3		60.9	83.37	93.57	6.43
	Blank				3.6	

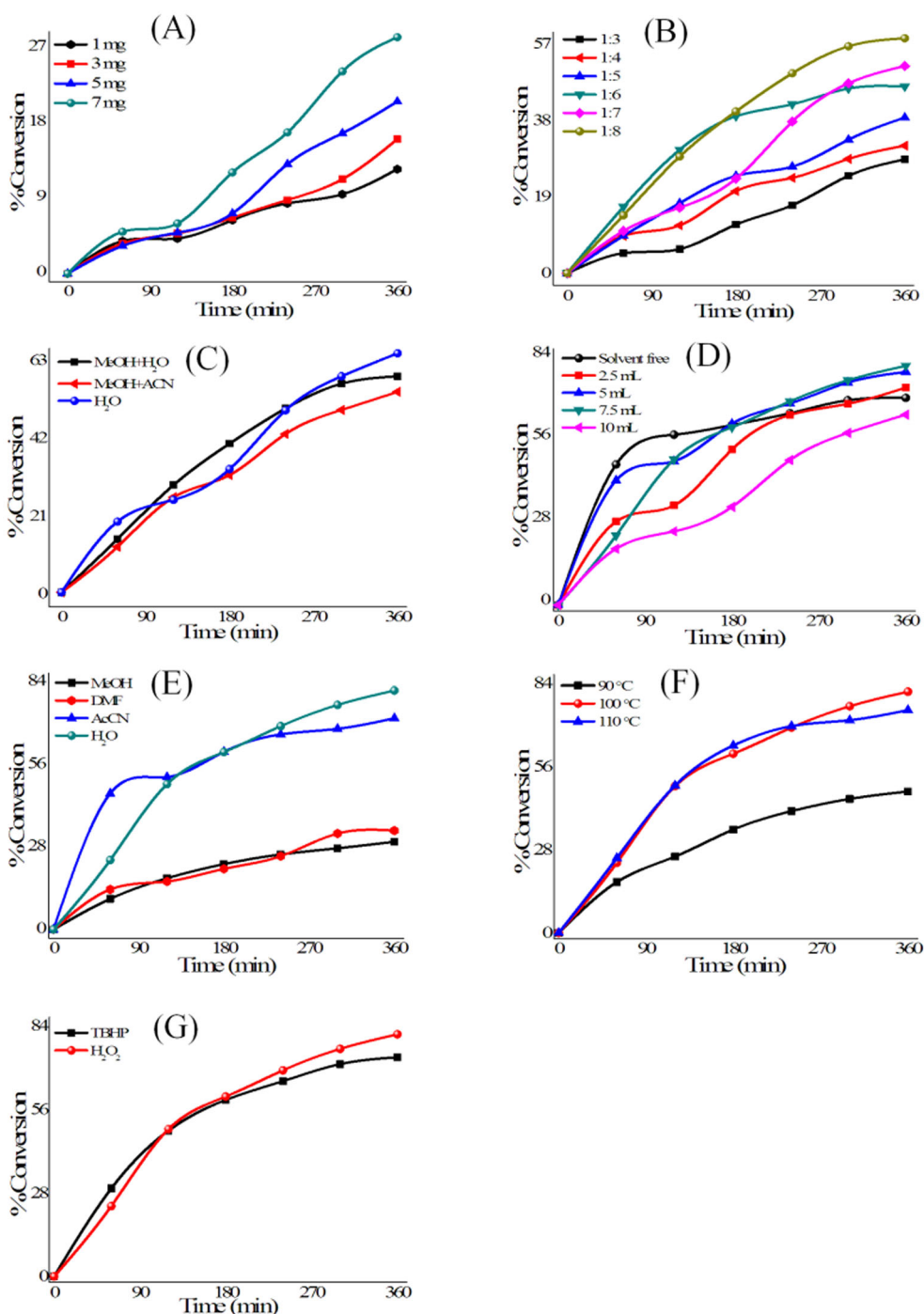


Figure 3. Optimization of reaction parameters for the oxidation benzyl alcohol in the presence of **3**: (A) variation of the amount of catalyst, (B) variation of H₂O₂ amounts, (C) variation of mixed solvent ratio, (D) variation of the solvent amount, (E) influence of types of solvent, (F) impact of temperature, (G) effect of type of oxidant.

Table 3. Data for all the parameters applied to optimize the oxidation of benzyl alcohol by H₂O₂ in the presence of **3**.

S. No.	Cat. (mg)	Oxidant	Subs: oxid.	Solv. (mL)	Solvent	Temp. (°C)	% Conv.	TON	TOF (h ⁻¹)
1	1	H ₂ O ₂	1:3	10	H ₂ O + MeOH	100	12.5	718.7	119.78
2	3	H ₂ O ₂	1:3	10	H ₂ O + MeOH	100	16.5	316.2	52.70
3	5	H ₂ O ₂	1:3	10	H ₂ O + MeOH	100	20.6	236.8	39.48
4	7	H ₂ O ₂	1:3	10	H ₂ O + MeOH	100	28.3	232.4	38.74
5	7	H ₂ O ₂	1:4	10	H ₂ O + MeOH	100	31.7	260.3	43.39
6	7	H ₂ O ₂	1:5	10	H ₂ O + MeOH	100	38.7	317.8	52.98
7	7	H ₂ O ₂	1:6	10	H ₂ O + MeOH	100	46.4	381.1	63.52
8	7	H ₂ O ₂	1:7	10	H ₂ O + MeOH	100	51.5	423.0	70.50
9	7	H ₂ O ₂	1:8	10	H ₂ O + MeOH	100	58.4	479.7	79.95
9	7	H ₂ O ₂	1:8	10	H ₂ O + AcCN	100	54.2	445.2	74.20
10	7	H ₂ O ₂	1:8	10	H ₂ O	100	64.6	530.6	88.43
11	7	H ₂ O ₂	1:8		Solvent free	100	70.3	577.4	96.24
12	7	H ₂ O ₂	1:8	2.5	H ₂ O	100	73.8	606.2	101.03
13	7	H ₂ O ₂	1:8	5	H ₂ O	100	79.1	649.7	108.28
14	7	H ₂ O ₂	1:8	7.5	H ₂ O	100	81.2	666.9	111.16
15	7	H ₂ O ₂	1:8	7.5	MeOH	100	29.8	244.7	40.79
16	7	H ₂ O ₂	1:8	7.5	DMF	100	33.6	275.9	45.99
17	7	H ₂ O ₂	1:8	7.5	AcCN	100	71.8	589.7	98.29
18	7	H ₂ O ₂	1:8	7.5	H ₂ O	110	75.0	616.0	102.67
19	7	H ₂ O ₂	1:8	7.5	H ₂ O	90	47.6	390.9	65.16
20	7	TBHP	1:8	7.5	H ₂ O	100	73.5	603.7	100.62

Oxidation of benzyl alcohol was also studied in different solvent systems, water + methanol (7 mL + 3 mL), water + acetonitrile (7 mL + 3 mL), and pure water (10 mL). With 64.6% substrate conversion(%), pure water appears to be the best in comparison to the other two solvent systems (shown in [Figure 3\(C\)](#)).

The effect of the solvent volume was also checked by using five different amounts of solvent, viz., 2.5 mL, 5.0 mL, 7.5 mL, 10 mL, and solvent free for the oxidation of benzyl alcohol in the presence of **3**. Increment in the volume of solvent from 2.5 mL to 7.5 mL causes a rise in substrate conversion(%) from 73.8% to 81.2% (shown in [Figure 3\(D\)](#)). Further increasing the volume of solvent from 7.5 mL to 10 mL drops the substrate conversion from 81.2% to 64.6%. Moreover, the solvent-free reaction condition does not improve the substrate conversion (70.3%) much. Thus, 7.5 mL of H₂O was considered as optimum. [Figure 3\(E\)](#) displays the impact of various types of solvents, MeOH, DMF, AcCN, and H₂O, and their polarity in the catalytic oxidation of benzyl alcohol (reaction conditions are mentioned in [Table 3](#)). Among the four solvents, methanol and DMF show lower substrate conversion of 29.8% and 33.6%, respectively. Water with 81.2% conversion exhibits the highest substrate conversion among the examined four solvents. Hence, clean and green H₂O was chosen as a solvent for the rest of the study.

The temperature was optimized by carrying out the catalytic reactions at 90, 100, and 110 °C while keeping the other reaction parameters fixed, and the result is displayed in [Figure 3\(F\)](#). With the rise in temperature from 90 to 100 °C, substrate increases from 47.6% to 81.2%, but at a higher temperature (110 °C), the conversion falls a few percent.

Entry number 14 in [Table 3](#) represents the optimized reaction conditions for the oxidation of benzyl alcohol in the presence of **3**, which are: 0.007 g of catalyst, 7.5 mL of H₂O, the substrate to oxidant ratio is 1:8, 100 °C temperature and 6 h.

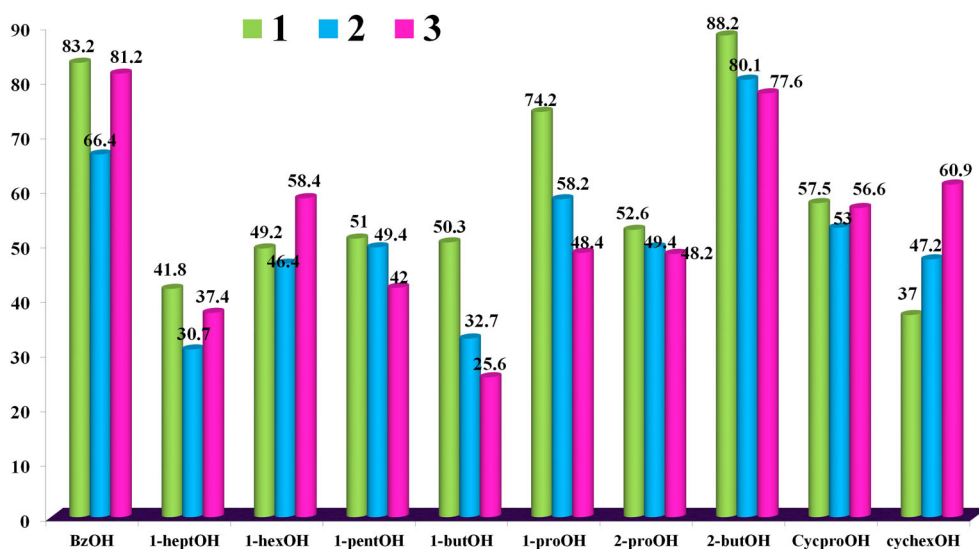


Figure 4. Comparison plots of substrate conversion (%) for the oxidation of alcohols in the presence of 1–3 under optimized reaction conditions.

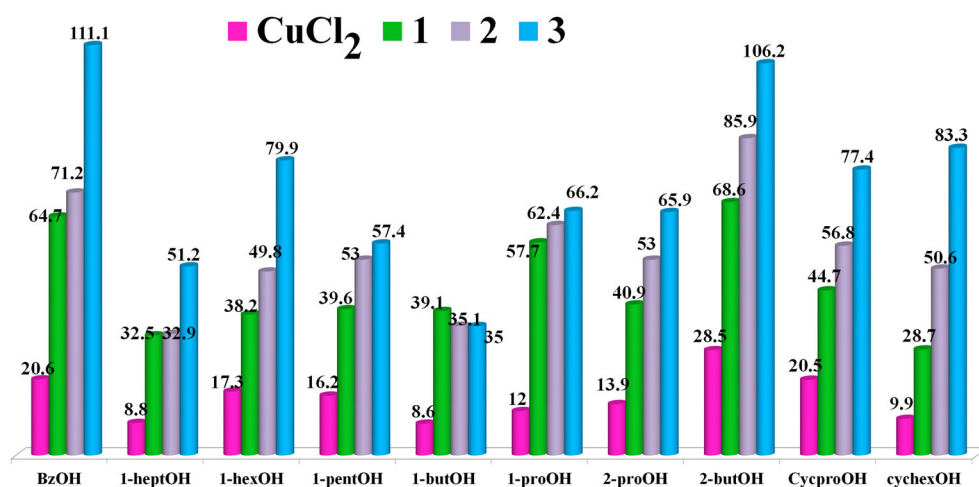
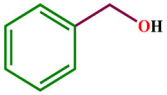


Figure 5. Comparison of TOF values for oxidation of alcohol in the presence of 1–3 and CuCl₂ under optimized reaction conditions.

The impact of oxidant was inspected by using TBHP in place of H₂O₂ under similar optimized reaction conditions, as mentioned above, and the result is shown in Figure 3(G). Clearly, TBHP shows comparable substrate conversion (73.5%) to H₂O₂ (81.2%). However, being an inexpensive and greener oxidant, hydrogen peroxide was the obvious choice for the oxidation of other alcohols under optimized reaction conditions.

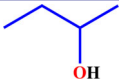
Under the optimized reaction conditions, the blank reaction of benzyl alcohol shows only 12.7% substrate conversion (Table 2), while **2** and **3** show 66.4% and 81.2% conversions, respectively. Oxidation of benzyl alcohol in the presence of **1–3** affords benzoic acid as a major product with nearly 80% selectivity. In terms of efficiency, with the TOF values of 111.16 h⁻¹, **3** is the best among the three catalysts studied here.

Table 4. Substrate conversion(%) and TOF values of catalytic oxidation of alcohols in the presence of 1–3 and contemporary catalytic systems.

S. No.	Cat.	Substrate	% Conv.	TOF (h ⁻¹)	Ref.	
1	1	 BzOH	83.2	64.72	Present work	
	2		66.4	71.27		
	3		81.2	111.16		
			[Cu ₂ (H ₂ O) ₂ (μ-L ²) ₂] (8)	52	–	[29]
			[Cu(H ₂ O)(L ³)] (9)	22	–	
			[Cu ₂ (L ₁)] (1 _{Cu})	34	98	[30]
			[Cu ₂ (L ₄)] (4 _{Cu})	75	401	
			[Cu((kNN'O-HL)(H ₂ O) ₂) (1)	33.4	167	[31]
			[Fe(kNN'O-HL)Cl ₂] (2)	26.7	133	
			[Fe(kNN'O-HL)Cl(μ-OMe) ₂] (3)	18.9	95	
	[Cu(OOC(C ₆ H ₅)Br)(C ₁₀ H ₉ N ₃)] (ClO ₄)	71	12	[32]		
2	1	 1-HeptOH	41.8	32.51	Present work	
	2		30.7	32.95		
	3		37.4	51.20		
			[Cu(OOCC(C ₆ H ₅) ₃)(bipy)(H ₂ O)](ClO ₄)(CH ₃ OH) (1)	12	–	[33]
			[Cu ₂ (OOCC ₆ H ₄ Br)(OCH ₃)(bipy) ₂ (ClO ₄) ₂] (3)	17	–	
			[Cu(OOC(C ₆ H ₅)Br)(C ₁₀ H ₉ N ₃)](ClO ₄)	13	2	[32]
			(Cu ₂ (OOCC ₆ H ₄ Br)(OCH ₃)(C ₁₀ H ₈ N ₂) ₂ (ClO ₄) ₂)	17	3	[34]
			[Cu(OOCC(C ₆ H ₅) ₃)(C ₁₀ H ₈ N ₂)(H ₂ O)](ClO ₄)(CH ₃ OH)	12.2	2	[35]
3	1	 1-HexOH	49.2	38.27	Present work	
	2		46.4	49.80		
	3		58.4	79.95		
			Cu0.1@Tannin-OMP	56	–	[36]
			Eu(NO ₃) ₃	72	–	[37]
	V ₂ O ₅ -Al ₁₃ nano hybrid	63.5	–	[38]		
4	1	 1-PentOH	51.0	39.67	Present work	
	2		49.4	53.02		
	3		42.0	57.49		
			K ₈ [BW ₁₁ O ₃₉ H] ₁₃ H ₂ O	38	–	[39]
			V ₂ O ₅ -Al ₁₃ nano hybrid	62	–	[38]
5	1	 1-ButOH	50.3	39.12	Present work	
	2		32.7	35.10		
	3		25.6	35.04		
			Cu0.1@Tannin-OMP	64	–	[36]
			PC-700	1	–	[40]
			TBAP	37	–	[41]
	[Cu ₃ (nph)(μ-Cl) ₂ (H ₂ O) ₆]·2H ₂ O	40	–	[42]		
6	1	 1-ProOH	74.2	57.71	Present work	
	2		58.2	62.47		
	3		48.4	66.26		
			[Cu ₃ (nph)(μ-Cl) ₂ (H ₂ O) ₆]·2H ₂ O	15	–	[42]
			Fe ₃ O ₄ @Ni-Co-BTC NPs (II)	30	–	[43]
7	1	 2-ProOH	52.6	40.91	Present work	
	2		49.4	53.02		
	3		48.2	65.98		
			Fe ₃ O ₄ @Ni-Co-BTC NPs (II)	25	–	[43]
			[Mo ^{VI} O ₂ {Hdfmp(bhz) ₂ }(MeOH)] (1)	94	–	[44]
			[Mo ^{VI} O ₂ {Hdfmp(inh) ₂ }(MeOH)] (2)	92	–	
			[Mo ^{VI} O ₂ {Hdfmp(nah) ₂ }(MeOH)] (3)	90	–	

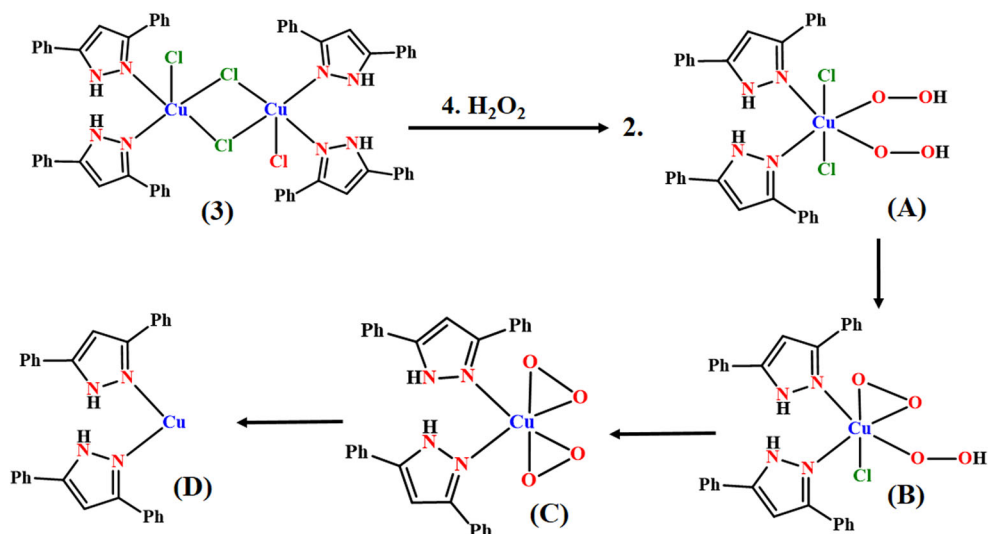
(continued)

Table 4. Continued.

S. No.	Cat.	Substrate	% Conv. TOF (h ⁻¹)		Ref.
8	1	 2-ButOH	88.2	68.61	Present work
	2		80.1	85.98	
	3		77.6	106.23	
	(Cu ₂ (OOCCH ₂ CH ₂ Br)(OCH ₃)(C ₁₀ H ₈ N ₂) ₂ (ClO ₄) ₂)		100	17	[34]
	Mn _x O _y /CeO ₂		41	–	[45]
	Mn _x O _y /ZrO ₂		51	–	
	Mn _x O _y /Al ₂ O ₃		51	–	
	Mn _x O _y /SiO ₂		55	–	
	[Mo ^{VI} O ₂ {Hdfmp(bhz) ₂ }(MeOH)] (1)		86	–	[44]
	[Mo ^{VI} O ₂ {Hdfmp(inh) ₂ }(MeOH)] (2)		87	–	
[Mo ^{VI} O ₂ {Hdfmp(nah) ₂ }(MeOH)] (3)	87	–			
Fe ₃ O ₄	82.5	–	[46]		
9	1	 CycproOH	57.5	44.72	Present work
	2		53.0	56.89	
	3		56.6	77.48	
	(Cu ₂ (OOCCH ₂ CH ₂ Br)(OCH ₃)(C ₁₀ H ₈ N ₂) ₂ (ClO ₄) ₂)		71	12	[34]
	HENU-1		50	–	[47]
[Pr ₄ (H ₂ O) ₆ (pzdc) ₂ As ₆ W ₅₈ O ₂₀₆] ³⁸⁻ (1 ^a)	50	–	[48]		
10	1	 CyhexOH	37.0	28.78	Present work
	2		47.2	50.66	
	3		60.9	83.37	
	[Cu((kNN'O-HL)(H ₂ O) ₂)] (1)		65.6	328	[31]
	[Fe(kNN'O-HL)Cl ₂] (2)		35.8	179	
	[Fe(kNN'O-HL)Cl(μ-OMe)] ₂ (3)		36.7	184	
	[Cu(OOCC(C ₆ H ₅) ₃)(bipy)(H ₂ O)][ClO ₄](CH ₃ OH) (1)		28	–	[33]
	[Cu(OOC(C ₆ H ₅)Br)(C ₁₀ H ₉ N ₃)](ClO ₄) (2)		29	–	
	[Cu ₂ (OOCCH ₂ CH ₂ Br)(OCH ₃)(bipy) ₂ (ClO ₄) ₂] (3)		53	–	
	[Cu ₂ (L ₁)] (1 _{cu})		38	157	[30]
	[Cu(OOC(C ₆ H ₅)Br)(C ₁₀ H ₉ N ₃)](ClO ₄)		29	5	[32]
(Cu ₂ (OOCCH ₂ CH ₂ Br)(OCH ₃)(C ₁₀ H ₈ N ₂) ₂ (ClO ₄) ₂)	53	9	[34]		
[Cu(OOCC(C ₆ H ₅) ₃)(C ₁₀ H ₈ N ₂)(H ₂ O)](ClO ₄)(CH ₃ OH)	28	4	[35]		

Carefully optimized reaction conditions were used to study oxidation of several other alcohols. In order to extend the scope of the catalysts, a total of 10 alcohols (five primary aliphatics, four secondary aliphatic, and one aromatic alcohol) were tested. Among the four aliphatic secondary alcohols, two are cyclic and two are acyclic or straight-chain alcohols. The detailed catalytic data of the alcohols are tabulated in Table 2.

Since aliphatic alcohols are hard to oxidize, **1–3** show excellent catalytic performance for oxidation of the studied alcohols. In the presence of **1**, all 10 alcohols, except 1-hexanol and cyclohexanol, show higher substrate conversion(%) compared to **2** and **3** (shown in Figure 4). Catalyst **3** exhibits higher substrate conversion(%) for the oxidation of 1-hexanol and cyclohexanol in comparison to the other two catalysts. Irrespective of the catalytic system, all the primary aliphatic alcohols produce the corresponding carboxylic acid as a major product. Selectivity(%) of carboxylic acid increases with decreasing carbon chain length of the aliphatic alcohols. Secondary aliphatic alcohols show preference toward corresponding aldehyde/ketone rather than the carboxylic acid. In all the cases, regardless of the catalytic system, nearly 100% product selectivity was observed during the oxidation of secondary aliphatic alcohols.



Scheme 2. Suggested reactive species generated *in situ* in the solution by the reaction of H_2O_2 with **3**.

Solubility of aliphatic alcohols in water decreases with an increase in carbon chain length. Thus the order of solubility of primary alcohols in water is 1-propanol > 1-butanol > 1-pentanol > 1-hexanol > 1-heptanol and the order of solubility for secondary alcohols is 2-propanol > 2-butanol > cyclopentanol > cyclohexanol. Due to partial solubility, alcohols maintain a constant concentration in water, which primarily decides the rate of the reaction [28]. Hence, it can be predicted that benzyl alcohol, 1-propanol, and 2-propanol will exhibit higher substrate conversion because they are miscible in water. Catalytic data also support this except for 2-propanol. The same trend of catalytic activity (based on the solubility of alcohols) can be observed for oxidation of primary and secondary alcohols in the presence of **1**. However, catalytic data of **2** and **3** do not obey the order of solubility consistently. Probably a second factor, other than solubility of the alcohol in water, influences the oxidation reaction. Nonetheless, alcohols with lower solubility display very good substrate conversion(%) in the presence of **1–3**.

Under optimized reaction conditions, oxidation of benzyl alcohol in the presence of **1–3** shows 83.2%, 66.4%, and 81.2% substrate conversion, respectively. Several reported homogeneous and heterogeneous catalytic systems [29–48] are far behind in terms of substrate conversion(%) as well as TOF values in comparison to **1–3** (Table 4). All three catalysts show excellent substrate conversion(%) for 2-butanol and display 88.2%, 80.1%, and 77.6% substrate conversion, respectively. The performance toward other aliphatic primary and secondary alcohols is not as good as for benzylic or 2-butanol. Still, the substrate conversion achieved for oxidation of aliphatic alcohols by **1–3** is significantly higher than contemporary catalytic systems [29–48]. A detailed comparison is shown in Table 4 with relevant catalytic systems.

All the catalysts show excellent TOF values for oxidation of listed alcohols. For comparison, catalytic oxidations of alcohols were also performed using CuCl_2 as catalyst. The TOF value comparison reveals (shown in Figure 5) that the efficiency of **1–3** is far superior to CuCl_2 , suggesting the active role of the ligands in **1–3** for catalytic

oxidation of alcohols. The control reaction of individual substrate exhibits less than 10% substrate conversion (shown in Table 2) under similar optimized reaction conditions.

In the current work, the detailed reaction mechanism for alcohol oxidation was not studied. However, the reaction mechanism for transition metal-catalyzed alcohol oxidation is well discussed in the literature [49]. By considering the reaction mechanism of alcohol oxidation of similar systems, it is suggested that initially the metal complex converts into the peroxy species by reacting with hydrogen peroxide. Thus, *in situ* generated metal peroxy complex regains its native form through oxidation of alcohols. A methanolic solution of H₂O₂ mixed with [Cu(DPPz)₂Cl₂]₂ (**3**) was analyzed through ESI-MS, and related data are displayed in Supplementary Figures S14 and S15. Scheme 2 shows various intermediate species identified *in situ* during the alcohol oxidation. The *m/z* values 641.04, 603.09, 567.11, and 503.16 are due to the formation of intermediate species **A**, **B**, **C**, and **D**, respectively. First, the dimeric copper(II) complex reacts with H₂O₂ in methanolic solution and converts into two units of monomeric copper(II) dihydroperoxido species (**A**), which readily converts into peroxy hydroperoxido species (**B**) by losing a labile chloride. Upon losing the second chloride from the molecule, (**B**) transforms into copper(II) diperoxy species (**C**). As expected, copper(II) diperoxy species (**C**) further undergoes decomposition, which leads to the formation of **D** as the base peak in the ESI-MS plot. Thus, three types of intermediate species form by adding H₂O₂ to solution of **3**. During the oxidation of alcohol, hydroperoxido species is considered solely responsible for oxidation of alcohol [7(c), 50]. However, current MS data indicate that along with the dihydroperoxido species (**A**), alcohol oxidation may also be influenced by intermediate species (**B**) and (**C**).

5. Conclusion

Pyrazole derivatives DMPz (**I**), MPPz (**II**), and DPPz (**III**) were prepared by an easy, clean, and straightforward pathway. Copper(II) complexes **1–3** oxidized various alcohols selectively with high substrate conversion and efficiency in comparison to most of the currently available homogeneous copper-based catalysts. Relatively more reactive, secondary aliphatic alcohols are highly selective (more than 92%) toward the formation of ketones, whereas both aromatic and aliphatic primary alcohols produce carboxylic acids as major products during the oxidation of alcohols in the presence of H₂O₂. Copper dihydroperoxido species (**A**) is suggested for the oxidation; however, influence from the other intermediate species (**B** and **C**) cannot be ignored. Catalysts **1–3** show excellent performance compared to contemporary catalysts. By considering the economic and environmental factors, the use of water as a green solvent and H₂O₂ as a green oxidant in the current work is an added advantage.

Acknowledgements

C.H. is very thankful to SAIF Mumbai for recording the TGA/DTA and EPR spectra. The authors also acknowledge CRF, IIT Ropar for ESI-MS data. The authors would like to thank CIF, IISER Bhopal, for the 400 MHz NMR facility. C.H. acknowledges CFR IIT(ISM) Dhanbad for providing single-crystal XRD analysis. A.M. is thankful to IIT (ISM) for fellowship. The GC and GC-MS used in

this study were procured from the grant given by the Science and Engineering Research Board (SERB), Department of Science and Technology (DST), grant no. SB/FT/CS-027/2014 and grant no. SB-EMEQ-055/2014, respectively, Government of India, New Delhi, India to C.H.

Disclosure statement

There are no conflicts of interest to declare.

Funding

C.H. thanks the Science and Engineering Research Board (SERB), Department of Science and Technology (DST), the Government of India, New Delhi for financial support [grant No. SB-EMQ-055/2014].

ORCID

Abhishek Maurya  <http://orcid.org/0000-0001-6977-9532>

Chanchal Haldar  <http://orcid.org/0000-0003-4642-7918>

References

- [1] A. Bocian, A. Gorczyński, D. Marcinkowski, S. Witomska, M. Kubicki, P. Mech, M. Bogunia, J. Brzeski, M. Makowski, P. Pawluć, V. Patroniak. *J. Mol. Liq.*, **302**, 112590 (2020).
- [2] D.B. Dess, J.C. Martin. *J. Org. Chem.*, **48**, 4155 (1983).
- [3] K. Omura, A.K. Sharma, D. Swern. *J. Org. Chem.*, **41**, 957 (1976).
- [4] K. Bowden, I.M. Heilbron, E.R.H. Jones, B.C.L. Weedon. *J. Chem. Soc.*, 39 (1946).
- [5] C. Djerassi. *Org. React.*, **6**, 207 (1944).
- [6] L.M.T. Frija, E.C.B.A. Alegria, M. Sutradhar, M.L.S. Cristiano, A. Ismael, M.N. Kopylovich, A.J.L. Pombeiro. *J. Mol. Catal. A: Chem.*, **425**, 283 (2016).
- [7] (a) J. Piera, J.E. Bäckvall. *Angew. Chem. Int. Ed. Engl.*, **47**, 3506 (2008). (b) H. Yang, Z. Ma, Y. Qing, G. Xie, J. Gao, L. Zhang, J. Gao, L. Du. *Appl. Catal. A*, **382**, 312 (2010). (c) J.U. Ahmad, M.T. Räisänen, M. Leskelä, T. Repo. *Appl. Catal. A: Gen.*, **411**, 180 (2012).
- [8] (a) S.S. Levos, H. Yuan, M.L.P. Collins, W.E. Antholine. *Curr. Topics Biophys.*, **26**, 43 (2002). (b) R.L. Liebermann, A.C. Rosenziolig. *Nature*, **434**, 177 (2005).
- [9] (a) M. Casavin, C. Corvaja, C.D. Nicola, D. Falcomer, I.L. Franco, M. Monair, L. Pandorfo, C. Pettinari, F. Piccinelli. *Inorg. Chem.*, **44**, 625 (2005). (b) R.K. Andrews, R.L. Blakely, Benner, In *Advances in Inorganic Biochemistry*, G.L. Eichhorn, L.G. Marzilli (Eds), Vol. 5, Elsevier, New York, 245 (1984).
- [10] (a) G. Mezei, R.G. Raptis, J. Teser. *Inorg. Chem.*, **45**, 8841 (2006). (b) T.E. Machonkin, H.H. Zhang, B. Hedman, K.O. Hodgson, E.I. Solomon. *Biochemistry*, **37**, 9570 (1998). (c) G.K. Mukhopadhyay, Z.K. Attich, P.L. Fox. *Science*, **279**, 714 (1998). (d) H.A. Regan, S. Nacht, G.R. Lee, C.R. Bishop, G.E. Cartwright. *Am. J. Physiol.*, **217**, 1320 (1969). (e) C.T. Huber, E. Frieden. *J. Biol. Chem.*, **245**, 3973 (1970).
- [11] (a) S. Osatav, D.A. Johnson. *J. Biol. Chem.*, **244**, 5757 (1969). (b) E.I. Solomon, U.M. Sundaram, T.E. Machonkin. *Chem. Rev.*, **96**, 2563 (1996). (c) G.N. Mukherjee, A. Das, *Elements of Bioinorganic Chemistry*, 4th Edn, U. N. Dhur & Sons, Private Ltd., Kolkata (1993). (d) D.C. Dalgarno, I.M. Armitage. *Adv. Inorg. Biochem.*, **6**, 113 (1984). (e) F.J. Carver, D.L. Farb, E. Frieden. *Biol. Trace Elem. Res.*, **4**, 1 (1982). (f) A.E. Palmer, L. Guintanar, S. Severance, T.P. Wang, D.J. Kosman, E.I. Solomon. *Biochemistry*, **41**, 9570 (2002).
- [12] D.S. Rozner, P.L. Alsters, R. Neumann. *J. Am. Chem. Soc.*, **125**, 5280 (2003).

- [13] (a) K. Sato, M. Aoki, J. Takagi, R. Noyori. *J. Am. Chem. Soc.*, **119**, 12386 (1997). (b) O. Bortolini, V. Conte, F. Di Furia, G. Modena. *J. Org. Chem.*, **51**, 2661 (1986). (c) C. Venturello, M. Gambaro. *J. Org. Chem.*, **56**, 5924 (1991). (d) Y. Ishii, K. Yamawaki, T. Ura, H. Yamada, T. Yoshida, M. Ogawa. *J. Org. Chem.*, **53**, 3587 (1988). (e) R. Neumann, M. Gara. *J. Am. Chem. Soc.*, **117**, 5066 (1995). (f) A. Berkessel, C.A. Sklorz. *Tetrahedron Lett.*, **40**, 7965 (1999). (g) J. Brinksma, M.T. Rispens, R. Hage, B.L. Feringa. *Inorg. Chim. Acta*, **337**, 75 (2002). (h) A.G.J. Ligtenbarg, P. Oosting, G. Roelfes, R.M. La Crois, M. Lutz, A.L. Spek, R. Hage, B.L. Feringa. *Chem. Commun.*, 385 (2001).
- [14] (a) M.L. Cheng, M.N. Qin, L. Sun, L. Liu, Q. Liu, X.Y. Tang. *Dalton Trans.*, **49**, 7758 (2020). (b) A.K. Dhara, K. Kumar, S. Kumari, U.P. Singh, K. Ghosh. *Transition Met. Chem.*, **45**, 159 (2020). (c) P.R. Verma, S. Payra, F. Khan, S. Penta, S. Banerjee. *ChemistrySelect*, **5**, 1950 (2020). (d) K. Sarma, N. Devi, M. Kalita, B. Sarma, P. Baraman. *J. Coord. Chem.*, **68**, 3685 (2015). (e) V. Thamilarasan, P. Revathi, A. Praveena, J. Kim, V. Chandramohan, N. Sengottuvelan. *Inorg. Chim. Acta*, **508**, 119626 (2020).
- [15] (a) M.H. Ardakani, S. Saeednia, P. Iranmanesh, B. Konani. *J. Inorg. Organomet. Polym.*, **27**, 146 (2017). (b) C.N. Kato, M. Hasegawa, T. Sato, A. Yoshizawa, T. Inoue, W. Mori. *J. Catal.*, **230**, 226 (2005). (c) S.N. Azizi, S.E. Tilami. *Microporous Mesoporous Mater.*, **167**, 89 (2013).
- [16] (a) M. Asthana, I. Syiemlieh, A. Kumar, R.A. Lal. *Inorg. Chim. Acta*, **502**, 119286 (2020). (b) S. Velusamy, T. Punniyamurthy. *Eur. J. Org. Chem.*, **20**, 3913 (2003).
- [17] (a) N. Barooah, S. Sharma, B.C. Sarma, J.B. Baruah. *Appl. Organomet. Chem.*, **18**, 440 (2004). (b) N. Zhao, D.M. Eichhorn. *Acta Cryst.*, **E61**, m822 (2005). (c) V. Chandrasekhar, S. Kingsley, A. Vij, K.C. Lam, A.L. Rheingold. *Inorg. Chem.*, **39**, 3238 (2000). (d) G. Mezei, R.G. Raptis. *Inorg. Chim. Acta*, **357**, 3279 (2004). (e) I.D. Giles, J.C. Depriest, J.R. Deschamps. *J. Coord. Chem.*, **68**, 3611 (2015). (f) B. Soltani, M.H. Sadr, J.T. Engle, C.J. Ziegler, S.W. Joo, Y. Hanifehpour. *Transition Met. Chem.*, **37**, 687 (2012).
- [18] F. Gosselin, P.D. O'Shea, R.A. Webster, R.A. Reamer, R.D. Tillyer, E.J. Grabowski. *J. Synlett*, **2006**, 3267 (2006).
- [19] R.H. Wiley, P.E. Hexner. *Org. Synth.*, **31**, 43 (1951).
- [20] T. Posner. *Ber.*, **34**, 3980 (1901).
- [21] D. Thiele. *Ann.*, **302**, 294 (1898).
- [22] Bertrand. *Compt. Rend.*, **245**, 2306 (1957).
- [23] N. Kitajima, K. Fujisawa, C. Fujimoto, Y. Morooka, S. Hashimoto, T. Kitagawa, K. Toriumi, K. Tatsumi, A. Nakamura. *J. Am. Chem. Soc.*, **114**, 1277 (1992).
- [24] B. Lee, P. Kang, K.H. Lee, J. Cho, W. Nam, W.K. Lee, N.H. Hur. *Tetrahedron Lett.*, **54**, 1384 (2013).
- [25] (a) G. Chattopadhyay, P.S. Ray. *Synth. Commun.*, **41**, 2607 (2011). (b) J. Safari, S.G. Ravandi. *Synth. Commun.*, **41**, 645 (2011). (c) F. Toda, S. Hyoda, K. Okada, K. Hirotsu. *Chem. Commun.*, 1531 (1995). (d) W. Tang, Y. Xiang, A. Tong. *J. Org. Chem.*, **74**, 2163 (2009). (e) X.H. Chen. *Acta Cryst.*, **E63**, o4443 (2007). (f) G.S. Chen, J.K. Wilbur, C.L. Barnes, R. Glaser. *J. Chem. Soc., Perkin Trans.*, **2**, 2311 (1995). (g) G.S. Chen, M. Anthamatten, C.L. Barnes, R. Glaser. *J. Org. Chem.*, **59**, 4336 (1994). (h) S.T. Heller, S.R. Natarajan. *Org. Lett.*, **8**, 2675 (2006).
- [26] (a) M.L. Jimeno, N. Jagerovic, J. Elguero. *Spectroscopy*, **13**, 291 (1997). (b) R.M. Claramunt, C. Lopez, M.A. Garcia, G.S. Denisov, I. Alkortac, J. Elguero. *New J. Chem.*, **27**, 734 (2003). (c) K. Gu, G. Yang, W. Zhang, X. Liu, Z. Yu, X. Han, X. Bao. *J. Organomet. Chem.*, **691**, 1984 (2006). (d) V.K. Aggarwal, J.D. Vicente, R.V. Bonnert. *J. Org. Chem.*, **68**, 5381 (2003).
- [27] (a) J.P. Donoso, C.J. Magon, J.F. Lima, O.R. Nascimento, E. Benavente, M. Moreno, G. Gonzalez. *J. Phys. Chem. C*, **117**, 24042 (2013). (b) M.R.M. Quijano, G.F. Sueta, M.F. Álamo, N.A. Alcalde, V.G. Vidales, V.M.U. Saldívar, L. Gasque. *Dalton Trans.*, **41**, 4985 (2012). (c) L. Gasque, V.M.U. Saldívar, I. Membrillo, J. Olguín, E. Mijangos, S. Bernès, I. González. *J. Inorg. Biochem.*, **102**, 1227 (2008). (d) L.G. Sebastián, V.M.U. Saldívar, E. Mijangos, M.R.M. Quijano, L.O. Frade, L. Gasque. *J. Inorg. Biochem.*, **104**, 1112 (2010). (e) G.M. Díaz, W.L. Driessen, J. Reedijk, S. Gorter, L. Gasque, K.R. Thompson. *Inorg. Chim. Acta*, **339**, 51 (2002). (f) E.J. Ukpong, N.W. Akpanudo, J. Prasad. *Afr. J. Pure Appl. Chem.*, **4**, 38 (2010). (g) S.

- Kumari, A.K. Mahato, A. Maurya, V.K. Singh, N. Kesharwani, P. Kachhap, I.O. Koshevoy, C. Haldar. *New J. Chem.*, **41**, 625 (2017). (h) E. Faggi, R. Gavara, M. Bolte, L. Fajari, L. Juliá, L. Rodríguez, I. Alfonso. *Dalton Trans.*, **44**, 700 (2015). (i) M. Lavanya, M. Jagadeesh, J. Haribabu, R. Karvembu, H.K. Rashmi, P.U. Maheswari, A.V.R. Devi. *Inorg. Chim. Acta*, **469**, 76 (2018). (j) A.J. Amoroso, M.W. Burrows, S.J. Coles, R. Haigh, R.D. Farley, M.B. Hursthouse, M. Jones, K.M.A. Malik, D.M. Murphy. *Dalton Trans.*, 506 (2008).
- [28] G.-J. ten Brink, I.W.C.E. Arends, R.A. Sheldon. *Science*, **287**, 1636 (2000).
- [29] M.N. Kopylovich, K.T. Mahmudov, M.F.C.G. da Silva, P.J. Figiel, Y.Y. Karabach, M.L. Kuznetsov, K.V. Luzyanin, A.J.L. Pombeiro. *Inorg. Chem.*, **50**, 918 (2011).
- [30] I. Timokhin, C. Pettinari, F. Marchetti, R. Pettinari, F. Condello, S. Galli, E.C.B.A. Alegria, L.M.D.R.S. Martins, A.J.L. Pombeiro. *Cryst. Growth Des.*, **15**, 2303 (2015).
- [31] M. Sutradhar, T.R. Barman, A.J.L. Pombeiro, L.M.D.R.S. Martins. *Catalysts*, **9**, 1053 (2019).
- [32] H. Ünver, I. Kani. *J. Chem. Sci.*, **130**, 33 (2018).
- [33] T.F.S. Silva, L.M.D.R.S. Martins. *Molecules*, **25**, 748 (2020).
- [34] H. Ünver. *Transit. Met. Chem.*, **43**, 641 (2018).
- [35] H. Ünver, I. Kani. *Polyhedron*, **134**, 257 (2017).
- [36] L. Kong, J. Zhao, S. Han, T. Zhang, L. He, P. Zhang, S. Dai. *Ind. Eng. Chem. Res.*, **58**, 6438 (2019).
- [37] S. Kim, Y. Kim, H. Jin, M.H. Park, Y. Kim, K.M. Lee, M. Kim. *Adv. Synth. Catal.*, **361**, 1259 (2019).
- [38] S. Wang, S. Li, R. Shi, X. Zou, Z. Zhang, G. Fu, L. Li, F. Luo. *Dalton Trans.*, **49**, 2559 (2020).
- [39] W. Zhao, Y. Zhang, B. Ma, Y. Ding, W. Qiu. *Catal. Commun.*, **11**, 527 (2010).
- [40] X. Hu, M. Fan, Y. Zhu, Q. Zhu, Q. Song, Z. Dong. *Green Chem.*, **21**, 5274 (2019).
- [41] Y. He, X. Ma, M. Lu. *Arkivoc*, **2012**, 187 (2012).
- [42] O.B. Chanu, A. Kumar, A. Lemtur, R.A. Lal. *Spectrochim. Acta A Mol. Biomol. Spectrosc.* **96**, 854 (2012).
- [43] A. Mohammadinezhad, B. Akhlaghinia. *Catal. Lett.* (2020). <https://doi.org/10.1007/s10562-020-03291-z>.
- [44] M.R. Maurya, S. Dhaka, F. Avecilla. *New J. Chem.*, **39**, 2130 (2015).
- [45] K. Prabu, M. Prabu, A.K. Venugopal, A.T. Venugopalan, W.V.Y.S. Sandilya, C.S. Gopinath, T. Raja. *Appl. Catal. A: Gen.*, **525**, 237 (2016).
- [46] F. Sadri, A. Ramazani, A. Massoudi, M. Khoobi, R. Tarasi, A. Shafiee, V. Azizkhani, L. Dolatyari, S.W. Joo. *Green Chem. Lett. Rev.*, **7**, 257 (2014).
- [47] D. Li, Q. Xu, Y. Li, Y. Qiu, P. Ma, J. Niu, J. Wang. *Inorg. Chem.*, **58**, 4945 (2019).
- [48] X. Ma, P. He, B. Xu, J. Lu, R. Wan, H. Wu, Y. Wang, P. Ma, J. Niu, J. Wang. *Dalton Trans.*, **48**, 12956 (2019).
- [49] (a) M.L. Chevallier, S. Dessolin, F. Serres, L. Bruyas, G. Chatel. *Molecules*, **24**, 4157 (2019). (b) A. Jia, L.L. Lou, C. Zhang, Y. Zhang, S. Liu. *J. Mol. Catal. A: Chem.*, **306**, 7 (2009). (c) O. Das, T.K. Paine. *Dalton Trans.*, **41**, 11476 (2012). (d) B.L. Ryland, S.D. McCann, T.C. Brunold, S.S. Stahl. *J. Am. Chem. Soc.*, **136**, 12166 (2014).
- [50] A.O. Kuzmin, G.L. Elizarova, L.G. Matvienko, E.R. Savinova, V.N. Parmon. *Mendeleev Commun.*, **8**, 210 (1998).